AENSI Journals

Australian Journal of Basic and Applied Sciences

ISSN:1991-8178

Journal home page: www.ajbasweb.com

ANFIS based Wind Speed Sensor-less MPPT Controller for Variable Speed Wind Energy Conversion Systems

[1]R. Sitharthan and [2]Dr. M. Geethanjali

[1]*Research scholar, Department of Electrical &Electronics Engg, Thiagarajar College of Engg, Anna university, Tamilnadu, India-625015.*
[2]*Assistant professor, Department of Electrical &Electronics Engg, Thiagarajar College of Engineering, Anna university, Tamilnadu, India--625015.*

ARTICLE INFO

Article history:
Received 19 August 2014
Received in revised form
19 September 2014
Accepted 29 September 2014
Available online 18 November 2014

Keywords:
Variable speed wind turbine, Doubly fed induction generator, Maximum power point tracking, Adaptive neuro-fuzzy inference system.

ABSTRACT

Background: Although, wind energy is abundant, it varies frequently throughout the day depending on the environmental conditions. Such frequent wind speed variation, makes the necessity of maximum power point tracking device in the Wind Energy Conversion System (WECS). The amount of power output from a WECS depends upon the accuracy with which the peak power points are tracked by the maximum power point tracking controller of the WECS control system irrespective of the variable speed generator used. **Objective:** To reduce the complexity in tracking the optimal power from a variable speed wind energy conversion system. A Adaptive Neuro-Fuzzy Inference System (ANFIS) based Maximum Power Point Tracking (MPPT) technique is proposed. **Results:** Compared to the existing technique, the proposed method reduces the complexity in leaning the peak power. Furthermore, the proposed method forecasts the optimal rotor speed of the wind turbine using the measured wind speed. Therefore, by regulating the optimal rotor speed, maximum power is extracted. **Conclusion:** We have proposed a simple and accurate technique to extract maximum power from a grid connected variable speed operated doubly fed induction generator based WECS. The optimal rotor speed of the wind turbine is estimated by the proposed MPPT technique. Therefore, maximum power is extracted from WECS for variable wind condition by dynamically adjusting the speed control loop of the rotor side converter.

To Cite This Article: R. Sitharthan and M. Geethanjali., ANFIS based Wind Speed Sensor-less MPPT Controller for Variable Speed Wind Energy Conversion Systems. ***Aust. J. Basic & Appl. Sci.,*** *8(18): 14-23, 2014*

INTRODUCTION

Wind energy conversion systems have developed into most abundant source renewable energy in the past decade. This has happened potentially due to the vast development in the production of lager wind generators as well as the advances made in power electronic systems and their function in extracting optimum wind power (Jamil., 1990). In the present decade, variable speed wind turbines are used more commonly than the fixed speed wind turbine because of their low wind capture, existence of mechanical stress and arise of power quality issues (Bhowmik and Spée, 1998). Furthermore, variable speed wind turbines are able to control and operate the wind turbines at its maximum power coefficient for a wide-ranging wind speeds. In addition to that, variable speed wind turbines have low aerodynamic noise and reduced mechanical stress. The power obtained from the wind flow is not stable; they vary frequently all through the day according to the environmental conditions. The extraction of maximum power from the wind turbine at certain wind speed depends upon the certain optimal value of rotor rotational speed (Reardon *et al*., 1990; Schiemenz and Stiebler, 2000). In order to use the wind energy system so economical and efficient, it is necessary to extract maximum available power from the wind. Therefore, MPPT control technique comes into existence in modern WECS. By means of MPPT controller, maximum possible power can be extracted by operating the wind turbine always in an optimal tip speed ratio (Camblong *et al*., 2006). The tip speed ratio of the wind turbine can be maintained at optimum value by operating the wind turbine at optimal rotor rotation speed.

The WECS can achieve maximum available power from the wind by means of the following methods, (i) The Hill Climb Searching (HCS) technique, (ii) Power Signal Feedback (PSF) technique and Tip Speed Ratio (TSR) technique. (Cárdenas and Peña, 2004; Datta and Ranganathan, 2003, Reardon *et al*., 1990). The HCS technique does not require wind speed data, generator rotor speed and the turbine characteristics. Furthermore, this technique works well only for very small wind turbine. In-case of large inertia wind turbine, the system

Corresponding Author: R. Sitharthan, Research scholar, Department of Electrical &Electronics Engg, Thiagarajar College of Engineering, Anna University, Tamilnadu, India-625015.
Tel: +91-9976679826; E-mail: sithukky@gmail.com

output power is installed with the turbine mechanical power and the rate of change in mechanically stored energy. This often renders the HCS technique ineffective (De Carlo *et al*., 1996; (De Battista et al., 2000)). In the PSF control technique, it is required to have knowledge on the wind turbines maximum power curves to track its maximum power through its control mechanism. Moreover, the power curves need to be obtained via simulation on individual wind turbine or data sheet of the wind turbine, which makes it difficult to implement with accuracy in practical application (Savaresi., 1999). The TSR control technique is so reliable control technique. That regulates the rotational speed of the generator to maintain the optimal TSR at which maximum power is extracted. The control method uses sensors to track the maximum power by regulating optimum rotor speed, thereby turbine torque can be controlled dynamically to maintain the TSR at an optimum value (Leithead., 1990; Kanellos and Hatziargyriou, 2002).

In this paper, a ANFIS based MPPT controller using the TSR technique for variable speed WECS is proposed. The proposed method of tracking maximum power uses sensor less system to measure wind speed. The proposed sensor less wind speed technique requires only the instantaneous active power as its input and estimates the wind speed. The estimated wind speed is used to determine optimal rotor speed. This optimal rotor speed is used to control the speed control loop of the rotor side converter. Thereby the turbine torque can be modified dynamically. This in-turn makes the turbine to operate at the optimum TSR value and maximize the output power. Furthermore, ANFIS based MPPT controller is designed by the combination of the sugeno fuzzy system and back propagation neural network to determine optimal power. Simulation is carried out in order to verify the performance of the proposed controller in a grid connected variable speed operated doubly fed induction generator (DFIG) based wind energy conversion system.

Modelling a DFIG based WECS:

a. Wind turbine system model:

A wind turbine converts wind power into mechanical power. The mechanical power generated by the wind turbine at the shaft can be expressed as (Burton *et al*., 2001),

$$P_m = 0.5\rho A C_p(\lambda,\beta)V^3 \tag{1}$$

Where ρ is the air density (typically 1.225 kg/m^3), β is the pitch angle (in degree), $C_p(\lambda,\beta)$ is the wind-turbine power coefficient (dimensionless), A is the swept area of the rotor blades (in m^2) and V is the wind speed (in m/s).

The turbine Power coefficient $C_p(\lambda,\beta)$, is the power extraction efficiency of the wind turbine. The equation is used to model $C_p(\lambda,\beta)$ based on the modelling turbine characteristics is shown below.

$$C_p(\lambda,\beta) = 0.5176\left(116*\frac{1}{\lambda_i} - \frac{2}{5}\beta - 5\right)e^{-\frac{21}{\lambda_i}} + 0.0068\lambda_i \tag{2}$$

Where, $1/\lambda_i = 1/(\lambda+0.08\beta)-(0.035/1+\beta^3)$. C_p is a nonlinear function of both tip speed ration (λ) and the blade pitch angle (β). Where λ is the ratio of the turbine speed (ω_r* R) to the wind speed (V) as follows.

$$\lambda = \frac{\omega_r^* R}{V} \tag{3}$$

Where ω_r is the rotational speed and R is is the radius of the swept area by turbine blades respectively.

$$T_m = \frac{P_m}{\omega_r} \tag{4}$$

The mechanical torque (T_m) is obtained from the values of mechanical power (P_m) and optimal rotor speed ω_r as given in equation (4).This is given as a source to the generator by means of gear shaft system. The shaft system is which modelled as a spring and a damper with a certain damping and stiffness coefficient values (Burton *et al*., 2001). The equation for the shaft system is given by,

$$\frac{dT_{tg}}{dt} = K_{tg}(\omega_t - \omega_r) \tag{5}$$

Where, T_{tg} is an internal torque model, D_{tg} is the damping coefficient of the coupling shaft between the two masses and K_{tg} is the shaft stiffness.

Figure 1 shows turbine mechanical power as a function of the tip speed ratio at various wind speeds. The power for a certain wind speed is maximum at a certain value of rotor speed called optimum rotor speed opt ω_r . This is the speed which corresponds to an optimum tip speed ratio opt λ. In order to have maximum possible power, the turbine should always operate at opt λ. This is possible by controlling the rotational speed of the turbine so that it always rotates at the optimum speed of rotation.

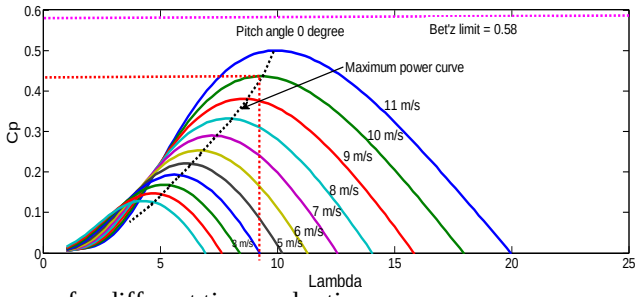

Fig. 1: Power co-efficient curve for different tip speed ratio.

b. DFIG system model:

By applying the parks transformation to the three-phase model of the DFIG it allows writing the dynamic voltages and flux equation in arbitrary d-q reference frame (Hofmann *et al*., 1997; Hofmann et al., 1997),

$$V_{ds} = R_s i_{ds} + \frac{d\psi_{ds}}{dt} - \omega_s \psi_{qs} \tag{5}$$

$$V_{qs} = R_s i_{qs} + \frac{d\psi_{qs}}{dt} - \omega_s \psi_{ds} \tag{6}$$

$$V_{dr} = R_r i_{dr} + \frac{d\psi_{dr}}{dt} - \omega_r \psi_{qr} \tag{7}$$

$$V_{qr} = R_r i_{qr} + \frac{d\psi_{qr}}{dt} - \omega_r \psi_{dr} \tag{8}$$

where R_s and R_r are the resistance of stator and rotor winding respectively, ω_s is the rotor revolving speed in synchronous orientation frame, $s\omega_s = \omega_s - \omega_r$ is the slip frequency, and the flux linkages are given by

$$\psi_{ds} = L_s i_{ds} + L_m i_{dr} \tag{9}$$

$$\psi_{qs} = L_s i_{qs} + L_m i_{qr} \tag{10}$$

$$\psi_{dr} = L_m i_{ds} + L_r i_{dr} \tag{11}$$

$$\psi_{qr} = L_m i_{qs} + L_r i_{qr} \tag{12}$$

where L_s, L_r and L_m are the stator leakage inductance, rotor leakage inductanceand the mutual inductance respectively. The electromagnetic torque equation of the DFIG is given by,

$$T_e = L_m (i_{qs} i_{dr} - i_{ds} i_{qr}) \tag{13}$$

The power losses associated with the stator resistance is neglected, then the active stator power (P_s) and reactive stator power (Q_s) delivered to grid are given by,

$$P_s = \frac{3}{2}(V_{ds} i_{ds} + V_{qs} i_{qs}) \tag{14}$$

$$Q_s = \frac{3}{2}(V_{qs} i_{ds} - V_{ds} i_{qs}) \tag{15}$$

DFIG WECS controller operation:

a. Rotor side converter control system:

A vector based control approach is used to control the rotor side converter in the rotor flux reference frame. The block diagram of the rotor side converter control is shown in figure 2. The proposed ANFIS based MPPT controller generates ω, the reference speed which, when set as the command speed for the speed control loop of the rotor side converter control system, maximum power points will be tracked by the WECS by dynamically changing the turbine torque to operate in opt λ. The essential d-q components of the rotor side converter voltage vector are derived from PI controlled speed controller and PI controlled current controller: These both controller functions to control the d-axis component and the q-axis component (Hilloowala and Sharaf, 1996; Kojabadi *et al*., 2004). For fast, forceful control capability voltage components are added to the direct and quadrature axis current regulator outputs respectively to form command d and q voltage. The d and q voltages are used as switching signals. Therefore, Space vector PWM generates the switching pulses for the converter power devices.

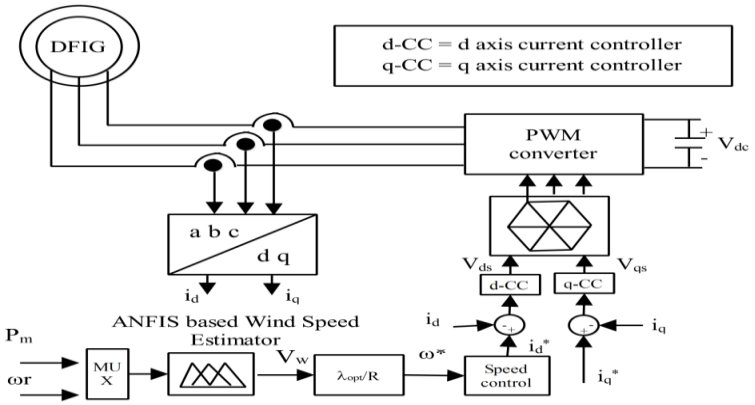

Fig. 2: Overall vector control of the RSC.

b. Grid side converter control system:

The grid-side converter power flow is controlled consecutively to keep up the dc-link voltage at reference value, 690 V. While, rising the output power to a certain extent than the input power to a dc capacitor causes a reduction of the dc- voltage and vice versa. The power output rotor will be regulated to keep dc- voltage more or less constant component (Kaura and Blasko, 1997; Kojabadi et al., 2004; Lee et al., 2000). The dc- voltage has been maintained at a constant value. Therefore, the reactive power flowing into the grid network has been controlled at zero value. The control block diagram of the grid side converter is shown in figure 3. This reactive power controlling is done via controlling the grid side converter currents using the d–q vector control approach. By aligning the q-axis of the reference frame along with the grid voltage position V_d= 0 and from equation (14) and (15) the active and reactive power can be modified and obtained as,

$$P_s = \frac{3}{2} V_{ds} i_{qs} \tag{16}$$

$$Q_s = \frac{3}{2} V_{qs} i_{ds} \tag{17}$$

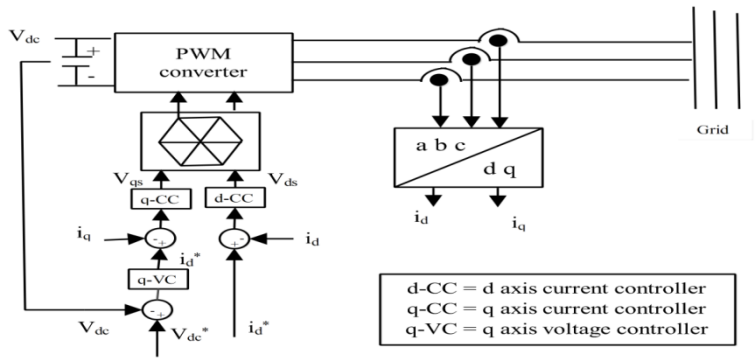

Fig. 3: Overall vector control of the GSC.

Real and reactive power control has been achieved by controlling d & q axis current components respectively. Controller uses two control loops to control the active and reactive power. They are, an outer dc-link voltage control loop is used to set the q-axis current reference for active power control. The inner control loop controls the reactive power by setting the d-axis current reference to zero value for unity power factor as shown in equation (17). The q-axis current is controlled to deliver the power flowing from the dc-link to the grid to maintain the dc-link voltage at constant value.

Maximum power point tracking control:

A sensor-less wind speed approximation based TSR control is modelled in-order to track the maximum power point of the WECS. The wind speed is approximated by using ANFIS. Furthermore, using the approximated wind speed and knowledge of opt λ, and opt ω_r command is executed. The opt ω_r command is applied to the speed control loop of the WECS (Wang and Chang, 2004). The PI controller controls the actual rotor speed to the desired value by varying the switching ratio of the PWM inverter. The control target of the inverter is the output power delivered to the load. The block diagram of the ANFIS-based MPPT controller

module is shown in figure 4. The inputs to the ANFIS are the rotor speed ω_r and mechanical power P_m. The P_m is obtained using the relation,

$$P_m = \omega_r\left(J\frac{d\omega_r}{dt}\right) + P_e \tag{18}$$

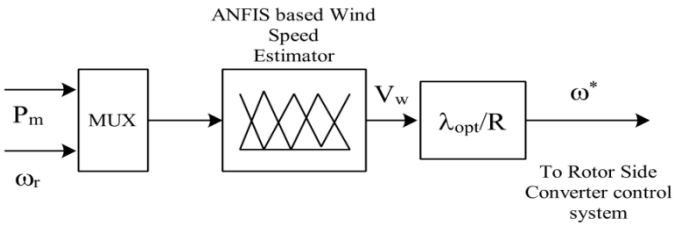

Fig. 4: ANFIS-based MPPT control module of turbine rotor speed.

a. Modelling a ANFIS based MPPT:

In this section, the estimation of the wind speed using the ANFIS concepts of is presented. The ANFIS is trained routinely by least-square inference and the back propagation algorithm. Figure 5 shows the structure of ANFIS with two inputs and one output. According to the designed model, the ANFIS network could make decision to estimate maximal wind speed based on the inputs/ outputs data used for training.

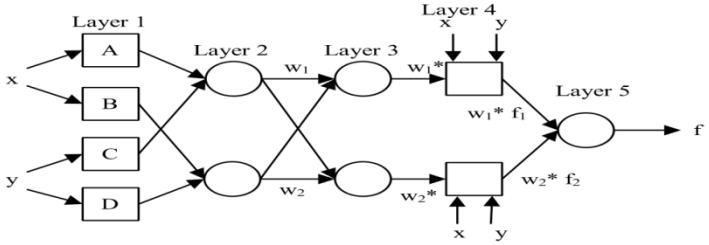

Fig. 5: Structure of ANFIS controller.

In this paper, ANFIS is examined with two inputs, rotor speed and mechanical power. The instantaneous wind speed is determined as the output from the ANFIS network. Furthermore, using the estimated wind speed and from equation (4) opt ω_r can be calculated. In this determination, the ANFIS first-order Sugeno model as well with fuzzy IF– THEN rules of Takagi and Sugeno's type is used If x is A and y is C then,

$$f_1 = p_1 x + q_1 y + r_1 \tag{19}$$

First layer:

This layer consists of two inputs, input 1 and input 2 as variables (MFs). This layer, transforms the input values x & y to the next layer and every node in this layer is considered as an adaptive node. In this study, bell-shaped MFs with maximum = 1 and minimum = 0 is selected.

Second layer:

The layer checks the weights of each MFs. It receives the input values from the 1st layer and acts as MFs to represent the fuzzy sets of the respective input variables. Every node in the second layer is non-adaptive and this layer multiplies the incoming signals and sends the product out like $w_i = \mu(x) * \mu(y)$. each node output represents the firing strength of a rule.

Third layer:

Each node (each neuron) in this layer performs the pre-condition matching of the fuzzy rules, i.e., they compute the activation level of each rule, the number of layers being equal to the number of fuzzy rules. Each node of these layers calculates the weights which are normalized. The third layer is also non-adaptive and every node calculates the ratio of the rule's firing strength to the sum of all rules' firing strengths like

$w_i^* = \frac{w_i}{w_1 + w_2}$, i=1,2. The outputs of this layer are called normalized firing strengths.

Fourth layer:

This layer is called the defuzzification layer and it provides the output values resulting from the inference of rules. Every node in the fourth layer is an adaptive node with node function

$O_i^4 = w_i^* xf = w_i^* (p_i x + q_i y + r_i)$ where, (p_i, q_i, r) is the parameter set and in this layer is referred to as consequent parameters.

Fifth layer:

This layer is called the output layer which sums up all the inputs coming from the fourth layer and transforms the fuzzy classification results into a crisp (binary). The single node in the fifth layer is not adaptive and this node computes the overall output as the summation of all incoming signals

$$\sum_i w_i^* f = \frac{\sum_i w_i f}{\sum_i w_i} \tag{20}$$

The hybrid learning algorithms were applied to identify the parameters in the ANFIS architectures. In the forward pass of the hybrid learning algorithm, functional signals go forward until layer 4 and the consequent parameters are identified by the least squares estimate. In the backward pass, the error rates propagate backwards and the premise parameters are updated by the gradient descent. The ANFIS based MPPT controller computes the optimum speed for maximum power point using information on the magnitude and direction of change in power output due to the change in command speed. The flow chart in figure 6 shows how the proposed MPPT controller is executed. The active power Po(k) is measured, and if the difference between its values at present and previous sampling instants ΔPo(k) is within a specified lower and upper power limits, PL and PM respectively then, no action is taken; however, if the difference is outside this range, then certain necessary control action is take as shown in figure 6.

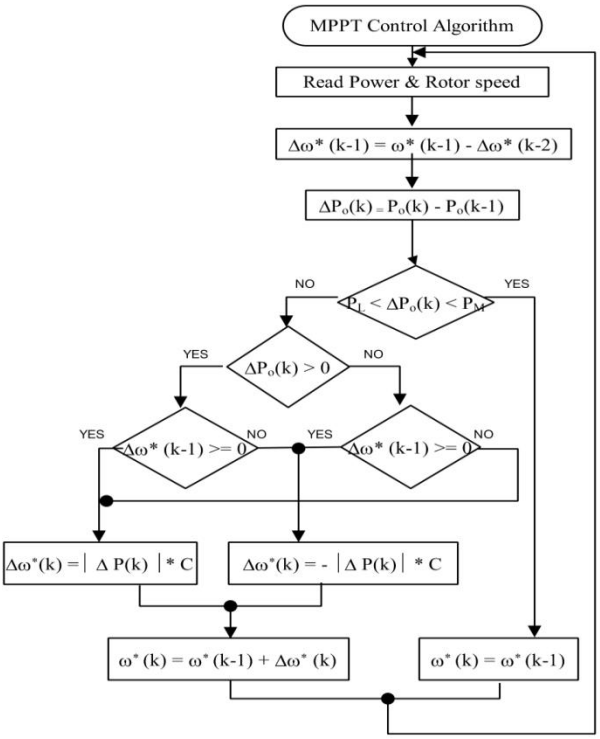

Fig. 6: Flow chart of MPPT controller.

RESULTS AND DISCUSSION

The proposed ANFIS based MPPT controller is analysed by means of 1 MW, grid connected variable speed operated DFIG based WECS. The complete grid connected WECS has been simulated using MATLAB/Simulink. The DFIG based WECS is connected to grid network by means of a back to back voltage source converter. Consequently, wind turbine and variable speed DFIG details are listed in Table 1. Consecutively, to analyse the performance of the proposed ANFIS based MPPT controller, the WECS is subjected to variable wind speed profile as listed in table 2. The wind flow is simulated as shown in figure 7 according to the furnished detail in Table 2. The wind speed details listed describe the flow of variable and uncontrollable wind speed during the month of April to October in southern region of Tamilnadu, India.

Table 1: Wind generation system parameters.

Parameter	Symbol	Value	Unit
Input wind speed	V	9-12	m/s
Mechanical output power	P_m	1.25	MW
Electrical output power	P_e	1	MW
System frequency	F	50	Hz
Line to line voltage	V_L	510	Volt
Rotor leakage inductance	L_r	0.133	p.u.
Stator resistance	R_s	0.0109	p.u.
Rotor resistance	R_r	0.0098	p.u.
Stator leakage inductance	L_s	0.140	p.u.
Magnetizing inductance	L_m	1.3	p.u.
Inertia constant	H	0.69	p.u.
No of pole pairs	P	2	-
Friction factor	F	0.01	p.u

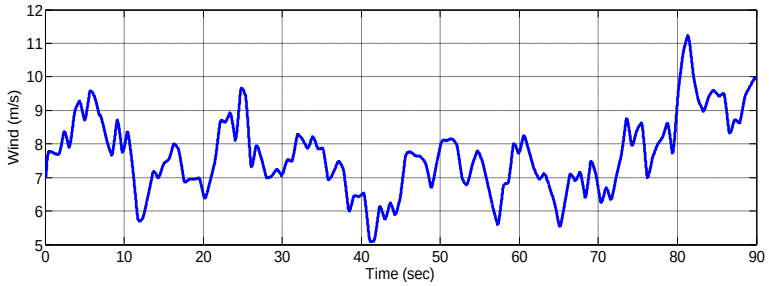

Fig. 7: Wind speed profile.

Table 2: Wind speed details.

Category	Wind speed details		
	Low wind session	Medium wind session	High wind session
Wind speed data (April - October)	3 to 4 m/s	5 to 8 m/s	9 to 12 m/s

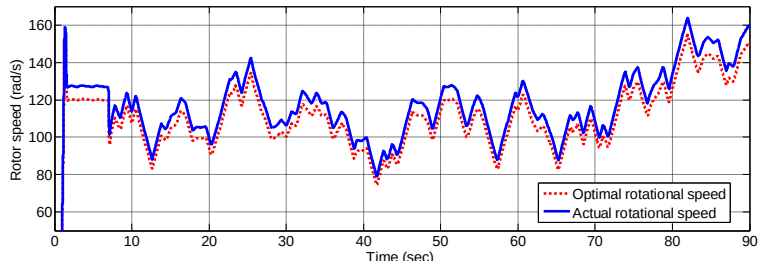

Fig. 8: Rotor rotational speed of the WECS.

In-order, to extract optimum power at variable wind speed condition, the wind turbine have to operate at λ opt. This is possible by controlling the rotor rotational speed of the WECS. So, it always operates at ωopt. Where, ωopt changes from a certain wind speed to another. The ANFIS controller is used to search the optimum rotational speed which tracks the maximum power point at variable wind speeds. On the other hand, figure 8 shows the variation of the actual and reference rotational speed as a result of the wind speed variation. At certain wind speed, the actual and reference rotational speeds are estimated and these values agree with the power characteristic of the wind turbine.

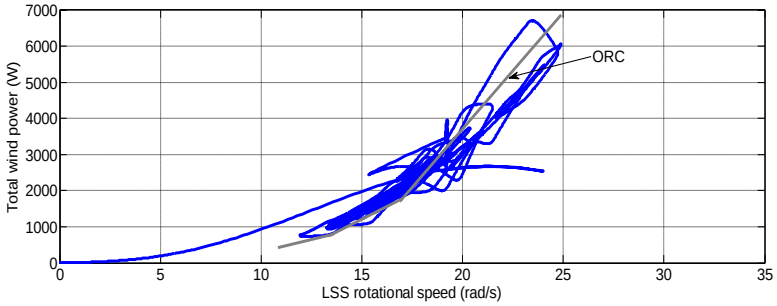

Fig. 9: Energy optimization achieving by tracking ORC.

As regards of the proposed MPPT controller, the rotor speed has been adjusted by steps of 0.5 rad/s: (every Ts=2s). Thereby, tracking performance of the proposed MPPT controller for the wind speed variation is obtained. Figure 9 shows the cyclic redundancy check (CRC) tracking performance for achieving energy optimization. Figure 10 presents a histogram of tip speed values in the same time interval, showing that values around the optimal one ($\lambda = 6$) appear the most often. The tip speed values have a standard deviation of σ_λ = 1.31 around a mean of λ_{opt} = 6.02. Figure 11 displays the corresponding evolution of the power coefficient. It can be observed that proposed MPPT controller achieves maximum power co-efficient of 0.475.

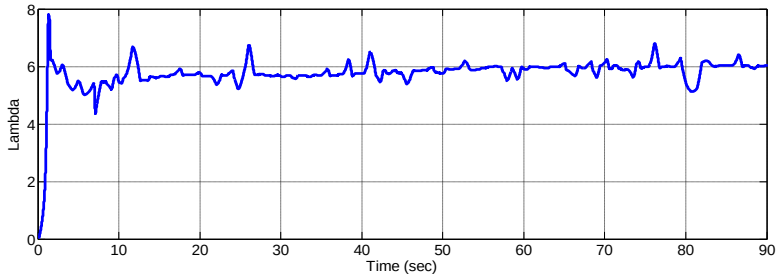

Fig. 10: Tip speed ratio of the WECS.

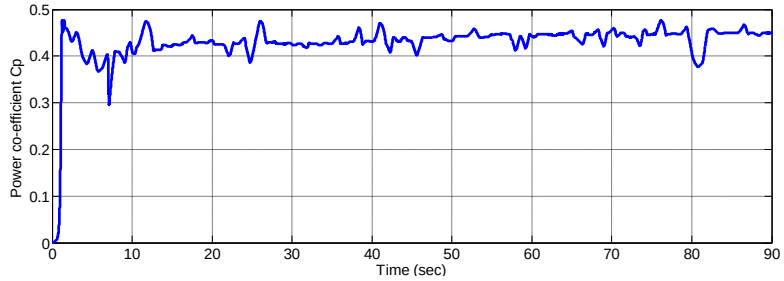

Fig. 11: Power co-efficient of the WECS.

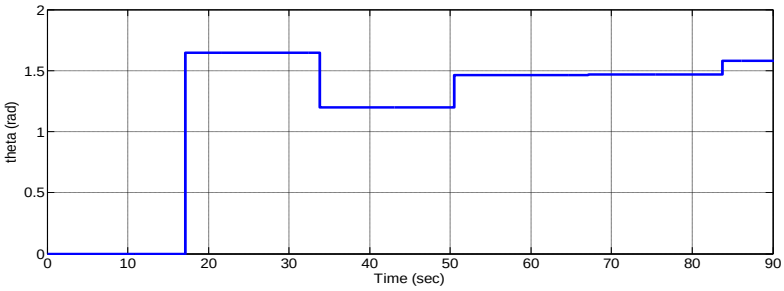

Fig. 12: Corresponding position signal, Θ.

Figure 12 presents the change in the Θ angle as the tip speed increases. In order to obtain this result, the rotational speed is imposed to vary in ramp between 20 rad/s and 250 rad/s, while the wind speed has an average component of 8 m/s and an indispensable turbulence component with medium intensity and constant statistical parameters. Furthermore, confirming the possibility of deciding the operating point's position relative to the optimal operating point, either at the left side if $\Theta < \pi/2$ or at the right side if $\Theta > \pi/2$. It is possible by controlling the rotational speed of the turbine so that it always rotates at the optimum speed of rotation. Figure 13 shows the characteristics curve of the proposed MPPT module, drawn between power co-efficient and TSR. Form the figure it can be noted that, for different wind speed and at particular rotor speed the power co-efficient is maximum. Power coefficient obtained is 0.475 and corresponding $\lambda = 6$.

Thus the power is maximized by the proposed controller and Performance comparison of the MPPT module in different models is shown in table 3. From the table it is observed that, different module is subjected to wind speed of 9 to 12 m/s and the computation time, power enhanced and mean square error (MSE) are analyzed. From the analysis, the proposed model has less computation time than the leithead model and Wang model. Furthermore, it enhances maximum power than the other module and MSE is found to be lower than the other module. From the analysis, the proposed MPPT model, performs better and extract maximum power from the wind.

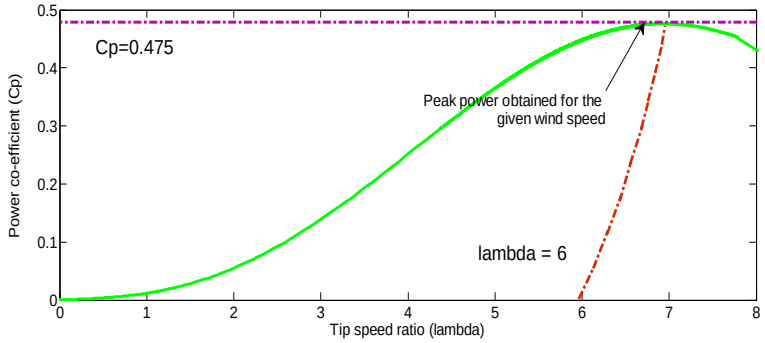

Fig. 13: Power co-efficient curve for different tip speed ratio obtained by proposed MPPT controller.

Table 3: Performance comparison of the MPPT module in different models.

Parameters / MPPT module	Wind speed m/s	Computation Time (Sec)	Maximum power enhanced (MW)	MSE
Proposed model	9 to 12	1.12	0.02	1.69×10^{-3}
Leithead model		1.45	0.0175	2.08×10^{-3}
Wang model		2.01	0.015	2.11×10^{-3}

Conclusion:

A wind speed measurement using sensor-less ANFIS based MPPT controller for variable speed based WECS was proposed. The proposed method does not require the knowledge of wind speed, air density or turbine parameters. The algorithm uses only the instantaneous active power and rotor speed to produce its output opt ω_r. This opt ω_r is fed as reference speed for the speed control loop of the rotor side converter controller enabling it to track the peak power points. The proposed method is analyzed in a grid connected variable speed operated DFIG WECS with a back-to-back voltage source converter. Results show good tracking capability by the proposed observer and the response of the system is found to be good. The MPPT controller proposed in this work is applicable to other types of WECS as well.

REFERENCES

Bhowmik, S. and R. Spée, 1998. Wind speed estimation based variable speed wind power generation. In: Proceedings of the Annual IEEE Conference of the Industrial Electronics Society – IECON'98: 596-601.

Burton, T., D. Sharpe, N. Jenkins and E. Bossanyi, 2001. Wind energy handbook. John Wiley & Sons, New-York.

Camblong, H., I. Martinez de Alegria, M. Rodriguez and G. Abad, 2006. Experimental evaluation of wind turbines maximum power point tracking controllers. Energy Conversion and Management, 47(18): 2846-2858.

Cárdenas, R. and R. Peña, 2004. Sensorless vector control of induction machines for variable speed wind energy applications. IEEE Transactions on Energy Conversion, 19(1): 196-205.

Datta, R. and V.T. Ranganathan, 2003. A method of tracking the peak power points for a variable speed wind energy conversion system. IEEE Transactions on Energy Conversion, 18(1): 163-168.

De Carlo, R.A., S.H. Zak and S.V. Drakunov, 1996. Variable structure, sliding-mode controller design. In: Levine WS (ed.) The Control Handbook, CRC Press, IEEE Press, 272: 941-951.

De Battista, H., P.F. Puleston, R.J. Mantz and C.F. Christiansen, 2000. Sliding mode control of wind systems with DFIG – Power efficiency and torsional dynamics optimization. IEEE Transactions on Power Systems, 15(2): 728-734.

Hansen, A.D., P. Sørensen, F. Iov and F. Blaabjerg, 2004. Control of variable speed wind turbines with double-fed induction generators. Wind Engineering, 28(4): 411-434.

Hilloowala, R.M. and A.M. Sharaf, 1996. A rule-based fuzzy logic controller for a PWM inverter in a standalone wind energy conversion scheme. IEEE Transactions on Industry Applications, 32(1): 57-65.

Hofmann, W., A. Thieme, A. Dietrich and A. Stoev, 1997. Design and control of a wind power station with double fed induction generator. In: Proceedings of EPE '97: 2723-2728.

Jamil, M., 1990. Wind power statistics and evaluation of wind energy density. Wind Engineering, 18(5): 227-240.

Kanellos, F.D. and N.D. Hatziargyriou, 2002. The effect of variable-speed wind turbines on the operation of weak distribution networks. IEEE Transaction on Energy Conversion, 17(4): 543-548.

Kaura, V. and V. Blasko, 1997. Operation of a phase locked loop system under distorted utility conditions. IEEE Transactions on Industry Applications, 33(1): 58-63.

Kojabadi, H.M., L. Chang and T. Boutot, 2004. Development of a novel wind turbine simulator for wind energy conversion systems using an inverter-controlled induction motor. IEEE Transactions on Energy Conversion, 19(3): 547-552.

Lee, D.C., G.M. Lee and K.D. Lee, 2000. DC-bus voltage control of three-phase AC/DC PWM converters using feedback linearization. IEEE Transactions on Industry Applications, 36(3): 826-833.

Leithead, W.E., 1990. Dependence of performance of variable speed wind turbines on the turbulence, dynamics and control. IEE Proceedings, 137(6): 403-413.

Reardon, D., S.A. De La Salle, W.E. Leithead and M.J. Grimble, 1990. Review of wind turbine control. International Journal of Control, 52(6): 1295-1310.

Savaresi, S.M., 1999. Exact feedback linearization of a fifth-order-model of synchronous generators. IEE Proceedings of Control, Theory and Applications, 146(1): 53-57.

Schiemenz, I. and M. Stiebler, 2000. Maximum power point tracker of a wind energy system with a permanent-magnet synchronous generator. In: Proceedings of ICEM 2000, 1083-1086.

Wang, Q. and L. Chang, 2004. An intelligent maximum power extraction algorithm for inverter based variable speed wind turbine systems. IEEE Transactions on Power Electronics, 19(5): 1242-1249.